

## HNPS Advances in Nuclear Physics

Vol 14 (2005)

HNPS2005



### Monte Carlo calculation of the response of He-3 counter with Geant4

*M. Manolopoulou, M. Fragopoulou, S. Stoulos, S. Petalas, M. Zamani*

doi: [10.12681/hnps.2266](https://doi.org/10.12681/hnps.2266)

#### To cite this article:

Manolopoulou, M., Fragopoulou, M., Stoulos, S., Petalas, S., & Zamani, M. (2019). Monte Carlo calculation of the response of He-3 counter with Geant4. *HNPS Advances in Nuclear Physics*, 14, 161–166.  
<https://doi.org/10.12681/hnps.2266>

# Monte Carlo calculation of the response of He-3 counter with Geant4

M. Manolopoulou, M. Fragopoulou, S. Stoulos, S. Petalas and M. Zamani

*Aristotle University of Thessaloniki, Physics Department, GR-54124, Greece*

---

## Abstract

Monte Carlo calculations with Geant4 were performed to calculate the response of He-3 proportional counters for neutrons of the energy region of 230 keV - 7 MeV. The results are compared with experimental data obtained by irradiation of the detectors with monoenergetic neutron beams produced by  ${}^7\text{Li}(p,n){}^7\text{Be}$  and  ${}^2\text{H}(d,n){}^3\text{He}$  reactions in the Tandem accelerator, NSCR Demokritos Athens.

---

## 1 Introduction

Helium filled proportional counters are widely used in the field of neutron detection and spectrometry [1, 2]. He-3 detectors are mainly utilized in measurements of thermal-epithermal neutrons, while they can be used for fast neutron measurements, but with limited efficiency. The response of helium counters to fast neutrons is usually calculated either by analytical techniques or by Monte Carlo methods. In this work He-3 counter was irradiated with mono-energetic neutron beams in the energy region from 230 keV - 7 MeV using the Tandem, Van de Graff accelerator facility at the Institute of Nuclear Physics, NSRF Demokritos, Athens, Hellas. The energy and resolution calibration of the detector was realized from the pulse height distributions obtained by these irradiations. The efficiency of the counter was calculated with Monte Carlo using Geant4. Finally, the experimental pulse height distributions were compared with the calculated spectrums.

## 2 Experimental

In this study a commercially available cylindrical He-3 counter was used. The effective length and diameter are 15 and 5 cm respectively. The gas mixture

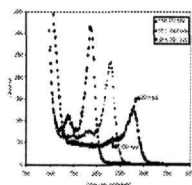


Fig. 1. Part of pulse height distributions obtained with He-3 counter. The two group of neutron energies that are emitted from  ${}^7\text{Li}(p,n){}^7\text{Be}$  and  ${}^7\text{Li}(p,n){}^7\text{Be}^*$  reactions are clearly distinguishable in each distribution.

consists from He-3, Kr and  $\text{CO}_2$  and the pressure is 6 atm. The measurement system consists of a high voltage power supply, a preamplifier suitable for proportional counters (Canberra model 2006), an amplifier (Tennelec model TC243 or Canberra model 2025) and a computer based multichannel analyzer (Tennelec PCA III or Canberra model Multiport II). Neutrons with energies in the range of 230 keV to 3.3 MeV were obtained via  ${}^7\text{Li}(p,n){}^7\text{Be}$  reaction. When the projectile energy is above 2.2 MeV, a second group of neutrons is emitted from  ${}^7\text{Li}(p,n){}^7\text{Be}^*$  reaction (0.429 MeV level) [3]. The peak due to  ${}^7\text{Li}(p,n){}^7\text{Be}^*$  reaction is clearly distinguishable from the peak of the main neutron group (Fig. 1), due to the energy difference between the neutrons emitted from these two reactions as well as due to the relatively smaller cross section of the second reaction. Thus, the second neutron group does not affect the measurements on the characteristic peak values of the main neutron group. As an example, in Figure 1 the two peaks corresponding to 2019 keV (due to  ${}^7\text{Li}(p,n){}^7\text{Be}$ ) and 1561 keV (due to  ${}^7\text{Li}(p,n){}^7\text{Be}^*$ ) are marked with arrows. Neutron energies in the range of 3.75 to 7.74 MeV were produced from  ${}^2\text{H}(d,n){}^3\text{He}$  reaction. Mean energy loss of the projectile energy in the target gas cell (Mo,  $5.1 \text{ mg}\cdot\text{cm}^{-2}$ ) was calculated using the SRIM/TRIM code [4]. The detectors were positioned parallel to the projectile beam direction at  $0^\circ$ . Due to the geometrical arrangement of the detectors with respect to the projectile beam direction and because of the openings of the detectors, neutrons with energies other than that of the  $0^\circ$  neutron energy also enter the detector volume (Fig. 2). In each of the irradiations the deviations from the  $0^\circ$  neutron energy and mean energies of the neutrons were calculated by weighting the neutron energies with their intensities at relevant directions. Angular dependences of laboratory cross sections and energies were calculated using the DROSG-2000 code, available from IAEA [5]. The difference between calculated mean neutron energies and the corresponding energies of neutrons at  $0^\circ$  varied from 0.1% to 0.3%.

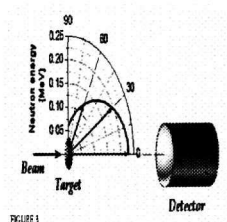


Fig. 2. Arrangement of the detector in respect to the beam direction. Neutron energy as a function of the emission angle is also presented for the case of  ${}^7\text{Li}(p,n){}^7\text{Be}$  reaction when proton energy is 2 MeV, as an example.

### 3 Results and Discussion

#### 3.1 Experimental results

Pulse height distributions obtained with He-3 counter during irradiations with neutrons via  ${}^7\text{Li}(p,n){}^7\text{Be}$  and  ${}^2\text{H}(d,n){}^3\text{He}$  reaction are presented in Fig. 3a and 3b. The pulse height distributions obtained with He-3 detector are composed of:

- (1) A peak due to the  ${}^3\text{He}(n,p){}^3\text{H}$  reaction, which will be referred as full energy peak. As the Q value of this reaction is 764 keV, the total kinetic energy of the reaction products is  $E_n + 764$  keV. A peak due to this energy is formed when both of the reaction products (i.e. p and  ${}^3\text{H}$ ) deposit all their energies within the detector volume. This peak appears towards the end of the pulse height distributions shown in Fig. 3. As the maximum proton energy that can be totally absorbed in this He-3 counter is about 7 MeV, the probability of registering pulses in full-energy peak decreases rapidly for neutrons above this energy because of increased probability of wall effects (Fig. 3b).
- (2) At neutron energies above 4.4 MeV a peak due to  ${}^3\text{He}(n,d){}^2\text{H}$  reaction. As the Q value of this reaction is -3.27 MeV, the total kinetic energy of the reaction products registered in the pulse height distributions is  $E_n - 3.27$  MeV.
- (3) A peak due to the recoiled  ${}^3\text{He}$  nuclei with recoil angle  $\theta_{lab} = 0^\circ$ , when all of their energy is deposited within the sensitive volume of the detector. The maximum energy,  $E_{max}$ , transferred to recoiled  ${}^3\text{He}$  nucleus, which travels in the direction of the incoming neutron, is  $E_n \cdot (4mM)/(m+M)^2 = 0.75 \cdot E_n$ , where  $E_n$  is neutron energy, M and m are the masses of  ${}^3\text{He}$  and neutron, respectively.
- (4) A continuum that originates from the recoiled  ${}^3\text{He}$  nuclei due to  ${}^3\text{He}(n,\text{elastic})$  reaction. In the absence of other phenomena, such as partially deposited energy due to wall effect or electronic effects, the expected shape of this

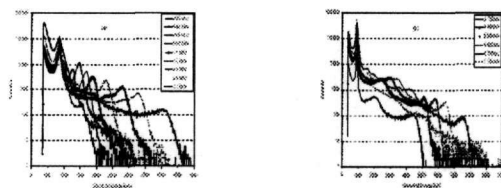


Fig. 3. Pulse height distributions obtained with He-3 counter during irradiations with neutrons via  ${}^7\text{Li}(p,n){}^7\text{Be}$  (a) and  ${}^2\text{H}(d,n){}^3\text{He}$  (b) reactions.

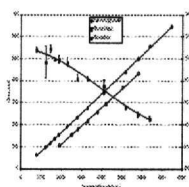


Fig. 4. The energy and the resolution calibration of He-3 counter.

continuum is the shape of the differential cross section,  $d\sigma(E_n)/d\Omega$ , of the  ${}^3\text{He}(n,\text{elastic})$  reaction [6].

- (5) A continuum due to the recoils of the other gasses present in the detector volume. The maximum energy of these recoils is significantly less than  ${}^3\text{He}$  recoil energy  $E_{\text{max}}$  i.e.  $0.05 \cdot E_n$  for Kr,  $0.29 \cdot E_n$  for C and  $0.22 \cdot E_n$  for O.
- (6) A peak due to the thermal-epithermal neutrons (764 keV). These low energy neutrons result from the neutron scattering by the material present in the irradiation hall (e.g. floor, walls, etc)
- (7) An exponentially decreasing component in the first part of the spectrum due to gamma ray interactions mainly with the detectors walls.

The experimentally obtained pulse height distributions are affected by other phenomena as well, such as statistical fluctuations in the gas amplification, recombination or electronic noise. In addition, depending on the gas pressure, the geometrical characteristics of the counter and reaction products direction, partial deposition of the latter kinetic energies within the detector volume can occur, while the rest is deposited in the detector wall (the wall effect). A fitting procedure was applied to the full energy and recoil peaks in the obtained pulse height distributions. The calculated energy and resolution calibration obtained is presented in Figure 4. The charge collected from  ${}^3\text{He}$  recoil nucleus is significantly smaller than the charge collected from proton and triton with the same total kinetic energy (see Fig. 4), mainly due to different ionization density and recombination effects.

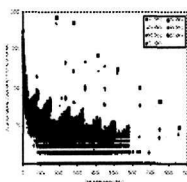


Fig. 5. Calculated spectra with different neutron beam energies. The full squares denote the full energy peak in each spectrum. In the above calculations the materials present in the experimental hall were not taken into account.

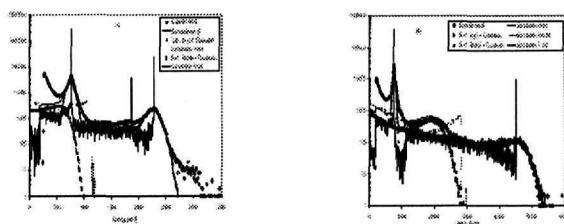


Fig. 6. Experimental and simulated pulse height distributions for neutron beam energies 1.51 MeV and 1.04 MeV (a) and 3.75 MeV (b). The simulated unfolded and folded spectra originating from different reactions are also presented.

### 3.2 Monte Carlo calculations

The response of He-3 counter was calculated using Geant4, with the physics lists provided for medical and military neutron applications. An accurate description of the detector geometrical characteristics and construction materials was provided. The angle-energy dependence of neutron beams was taken into account (see Fig.2). Detector support and the major volumes present in the experimental hall were also described. With the above input the total energy deposited into the detector gas mixture was calculated, Figure 5. The events originated from different reactions ( $^3\text{He}(n,p)^3\text{H}$ ,  $^3\text{He}(n,\text{elastic})$  and  $^3\text{He}(n,d)^2\text{H}$ ) were separated and treated with the corresponding energy calibration (see Fig.4). Finally the calculated spectra were folded with Gaussian distribution according to the experimentally determined resolution calibration. Preliminary results presented in Figure 6, show good correlation between the experimental and calculated spectra.

Finally, the experimental data obtained via  $^7\text{Li}(p,n)^7\text{Be}$  reaction (neutron energies from 230 keV to 3.3 MeV) were used to calculate the full energy peak efficiency according to the energy dependent reaction cross section, i.e. (counts recorded in full energy peak)/(neutrons emitted via  $^7\text{Li}(p,n)^7\text{Be}$  reaction during irradiation). In order to take into account the influence of other factors such as geometrical arrangement, uncertainties in target mass etc., the data were normalized to one calculated data point via Geant4. The results presented in

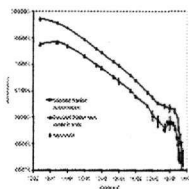


Fig. 7. Calculated and experimentally determined efficiency of He-3 counter to fast neutrons. The point that corresponds to thermal neutrons is provided by the manufacturer of the counter.

Figure 7 are in acceptable agreement with the calculated ones.

#### 4 Conclusions

Linear response with neutron energy was observed for He-3 counter when it is irradiated parallel to the anode wire. He-3 counter studied in this work can be effectively used for neutron spectroscopy up to 7 MeV. The resolution of the counter was in the range of 4-11% for the full energy peak. Preliminary calculations performed by Monte Carlo method using Geant4 to simulate the response of He-3 to fast neutrons are in acceptable agreement with the experimentally determined one.

#### References

- [1] E.Dietz, M. Matzke, W.Sosaat, G.Urbach and M.Weyrauch, Nucl. Inst. Meth. In Phys. Research A 332 (1993) 521-528.
- [2] M.Weyrauch, A.Casnati, P.Schillebeeckx and M.Clapham, Nucl. Inst. Meth. In Phys. Research A 403 (1998) 442-454.
- [3] C.A.Uttley, Neutron Physics and Nuclear data in Science and Technology, vol. 2, Neutron Sources for Basic Physics and Applications, an OECD/NEA report, Pergamon 1983.
- [4] J. F. Ziegler, J. P. Biersack, U. Littmark, Stopping and Ranges of Ions in Matter, Pergamon Press, New York (1985). See also: SRIM/TRIM The Stopping and Range of Ions in Matter. [www.srim.org](http://www.srim.org)
- [5] DROSG-2000: Neutron Source Reactions, Data files with computer codes for 57 accelerator-based neutron source reactions. Version 2.2 (January 2003). M. Drog, Institute for Experimental Physics, University of Vienna, Austria.
- [6] G.F.Knoll, Radiation Detection and Measurement, Third Edition, John Wiley & Sons, Inc. New York 1999.